



Feasibility of Modifying Coal Pillars to Prevent Sand Flow Under a Thick Loose Layer of Sediment and Thin Bedrock

Zhongbo Yu¹ · Shuyun Zhu¹ · Yunzhang Guan² · Dongxiang Hu²

Received: 12 December 2017 / Accepted: 31 July 2019 / Published online: 5 August 2019
© Springer-Verlag GmbH Germany, part of Springer Nature 2019

Abstract

This paper focuses on the first work face under a thick loose layer of sediment and thin bedrock in the No. 8 Mining District of the Baodian Coal Mine in the Yanzhou mining area of China. Due to mining, the hydrogeological conditions in the aquifers at the bottom of the thick, loose sediment layers have been greatly changed in the shallow areas in this area. The main problem is a low-pressure, water-rich aquifer. However, this problem could be remedied by modifying the coal pillars to prevent sand flow instead of water seepage. To do so, measurements of the first work face were obtained from drilling data, and the stress distribution and plastic zone were determined by examining the mining of the upper part of the no. 3 coal seam using FLAC^{3D} numerical analysis software. The simulated results were also compared with the empirically calculated results. Comprehensive analysis indicates that modifying the coal pillars from preventing water seepage or inrush to preventing sand flow appears feasible, and provides an important reference for increasing mining areas and recovery of coal resources.

Keywords Numerical simulation · First work face

Introduction

Coal is formed in sedimentary strata, and after mining, two zones form that are closely related to the water flow: a caved zone and a water-flow fractured zone (hereinafter referred to as the “Two Zones”). When the height of the immediate roof strata is between that of the Two Zones, the bedrock is generally called ‘thin bedrock’. If the height of the bedrock exceeds that of the water flow fractured zone, it is called ‘conventional bedrock’. Finally, if the height of the bedrock is less than that of the caved zone, the bedrock is known as ‘very thin bedrock’ (Fang et al. 2007; Palchik 2002; Yang and Xia 2013). Here, the focus is on the first work face under a thick, loose layer of sediment and thin bedrock in the Baodian Coal Mine of the Yanzhou mining area in eastern China.

The thick, loose soil layers in eastern China are usually composed of Quaternary and Neogene sediments, with a thickness exceeding 100 m. Generally, the loose sediments comprise sand, clay, and gravel (Feng et al. 2011; Hang et al. 2009; Zhao et al. 2017). The loose sediment layer contains an interactive sequence of aquifers and aquicludes. Typically, a 13 m thick aquifer is found at the bottom of the sediment layer. This aquifer is often referred to as a “bottom aquifer” (Lu and Wang 2015; Zhang et al. 2010). A water-flow-fractured zone that extends to the bottom aquifer could cause an inrush (Jin et al. 2011; Li and Chen 2016; Wu et al. 2011, 2016), but, since the bottom aquifer is only under low pressure, the coal pillar does not have to be as massive to prevent water inrush. However, the pillar still needs to be able to confine the bottom aquifer (Baumann et al. 2017; Bertuzzi et al. 2016; Liu et al. 2009; Xu et al. 2016).

The Yanzhou mining area has thick, loose layers of sediment (Wu et al. 2000; Sun et al. 2015). Due to the duration of mining, the water level in the aquifer at the bottom of the thick, loose layer of Cenozoic rock has changed, and there is typically little or no hydrostatic pressure. This means that the original 80 m coal pillars in the Baodian Coal Mine are now overly conservative, leaving a large volume of unmined, high-quality coal. Since the bottom aquifer has little or no pressure, it appeared

✉ Shuyun Zhu
shyzhuqiao@163.com

¹ Institute of Mine Water Hazards Prevention and Controlling Technology, School of Resources and Geosciences, China University of Mining and Technology, Xuzhou 221116, Jiangsu, China

² Yanzhou Coal Mine Co., Yankuang Group, Zoucheng 273500, China

reasonable to redesign the coal pillars to prevent sand flow (Bense et al. 2003; Poulsen et al. 2014; Waclawik et al. 2016; Wei et al. 2017; Wen et al. 2013), thus allowing more coal to be mined. A preliminary estimate of the increase in recoverable coal reserves totaled 18,749,000 t, which would have significant economic and social benefits (Liu and Guo 2000; Reed et al. 2017; Zhang et al. 2017; Zhu et al. 2014). Therefore, we determined the feasibility of establishing a coal pillar to prevent sand flow, while still protecting the first work face of the no. 3 coal seam of the No. 8 Mining District in the Baodian Coal Mine.

Geological Background

Basic Conditions of First Work Face

Geological background information for the Baodian Coal Mine, which is located in Zoucheng City, Shandong Province, is provided in Fig. 1a. The first working face, which is called 83-01, is found in the south end of the mine and was the initial workface in this area (Fig. 1b). The wall of the open cut (otherwise known as the pit slope) is designed to the south of 83-01. The thickness of the coal seam ranges from 4.96 to 6.60 m, with an average of 5.78 m. The eastern and western regions are the 83-02 and 83-03 workfaces, which have not yet been mined.

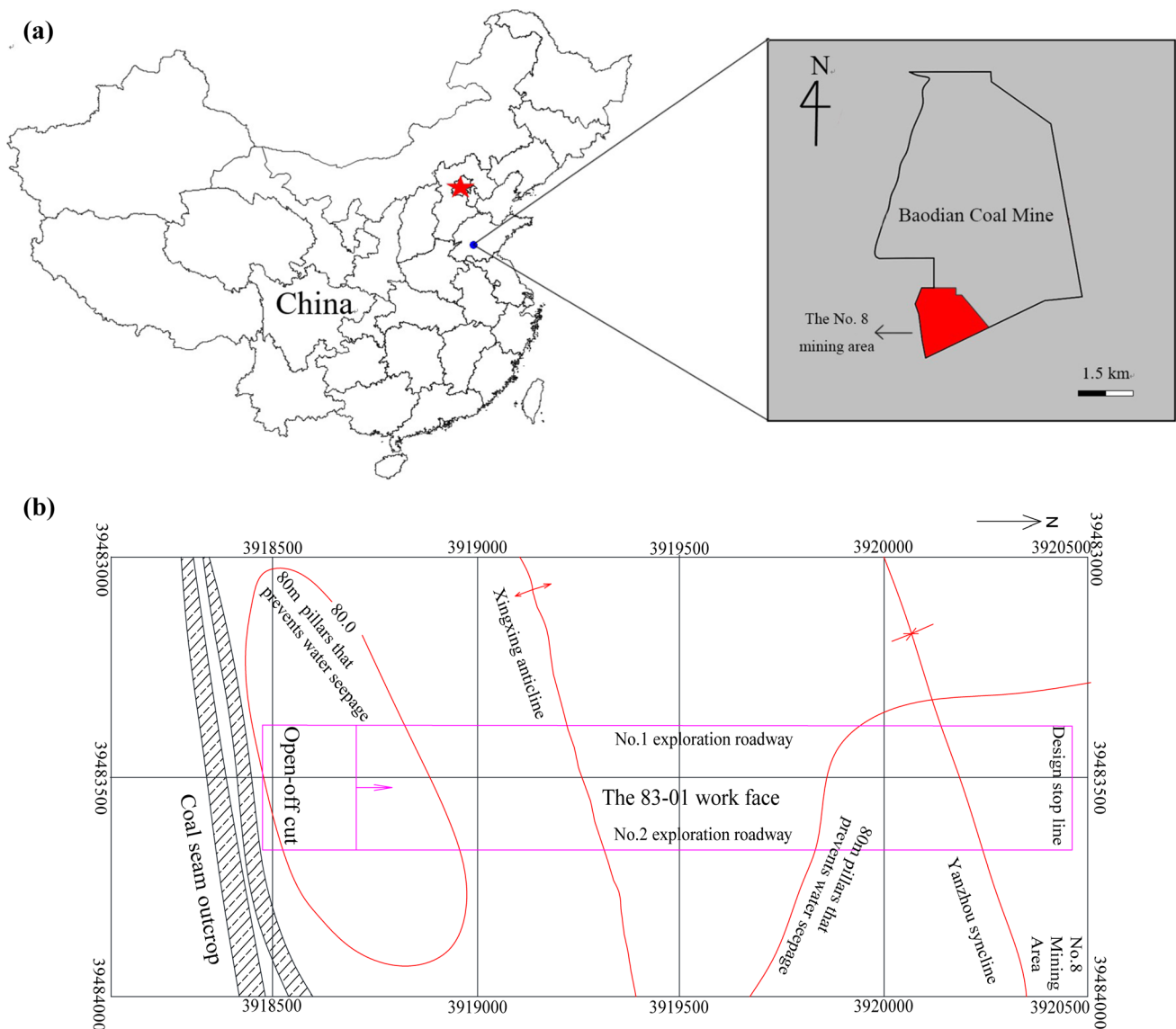


Fig. 1 The No. 8 Mining District in Baodian coal mine: **a** geographic location of the Baodian coal mine; **b** layout of first work face

The 83-01 workface is ≈ 1980 m long, with an inclined width close to 280 m; the elevation of the floor at the workface is -145 m to ≈ -260 m. Since the coal seam on the workface is affected by the fold structure, the orientation of the coal seam is obviously changed. The coal seam strike is $0^\circ-179^\circ$, and the dip direction is $90^\circ-359^\circ$ (azimuth). The dip of the coal seam is $5^\circ-19^\circ$, with an average of 11° . Near the drilling of O₂-13, which is south of the workface, the maximum dip of the deposit is approximately 19° . A gentle anticline exists in the south, where a tectonic basin has developed south of the workface; and the Xingxing anticline, which points axially northeast at 65° , lies in the middle of the workface. North of the workface, the Yanzhou syncline points axially northeast at 50° and pivots towards the northeast.

Characteristics of Overlying Rock and Soil

Two primary aquifers occur in the overlying rock and soil. The upper aquifer is found gravel rock of the Upper Jurassic (“the red layer”), while the bottom aquifer is situated thick loose Quaternary sediment (Fig. 2).

According to the results of a hydrogeological supplementary survey of the No. 8 Mining District in 2016, the inflow rate from pumping tests conducted near the red layer at two test locations was 0.00192 and 0.01785 L/s, while the corresponding permeability coefficients (k) was 0.0068 and 0.00258 m/day, respectively. These results indicate a water-poor aquifer. This is because the red layer is affected by long-term excavation and drainage of the No. 4 Mining District on the eastern side of the mine, which affected the water supply so that the water level was drastically reduced. At present, the water head is 44.77–58.19 m high, much lower than in 2013, and generally exhibits little or no pressure. The changes in the water level are obvious (Fig. 3).

The authors have also performed pumping tests for the bottom aquifer and found that the aquifer contains little water. The inflow rate was 0.021584 and 0.030224 L/s for the two tested locations.

The first exploration roadway is in the thinnest part of the bedrock according to an analysis of the drilling data. Figure 4a provides a cross-section of the surface stratigraphy, in which the overlying height of the bedrock is found along the first exploration roadway. The geological layer appears to fluctuate and the roof of the coal seam slopes downwards at the centre of the Xingxing anticline, with the lowest thickness measuring 31.26 m and occurring ≈ 750 m from the wall of the open cut. The maximum thickness of the bedrock is ≈ 90 m, which occurs at the end of the underground mine. This value is considered the normal thickness of the bedrock.

The contrasts among the heights of the bottom clay layer, bedrock, and coal seam roof in the first exploration roadway

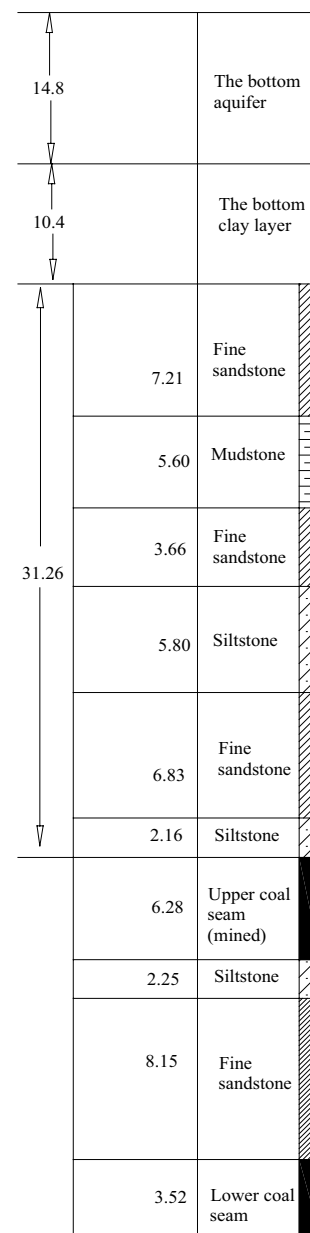


Fig. 2 Stratigraphic lithology profile

are shown in Fig. 4b. A comparison shows that the bedrock overlying the coal seam is clearly thinnest at 31.26 m in the core of the anticline and occurs in this area because of the influence of the Xingxing anticline. However, correspondingly, the thickness of the bottom clay layer is the greatest, which can prevent the water-flow-fractured zone from increasing in size. Moreover, the area that has a thinner layer of bottom clay has relatively thick bedrock. The lowered water levels and water exhaustion of the bottom aquifer are basic issues that can be used to modify the coal pillars from those that prevent water seepage to those that prevent sand flow.

Fig. 3 Changes in water elevation

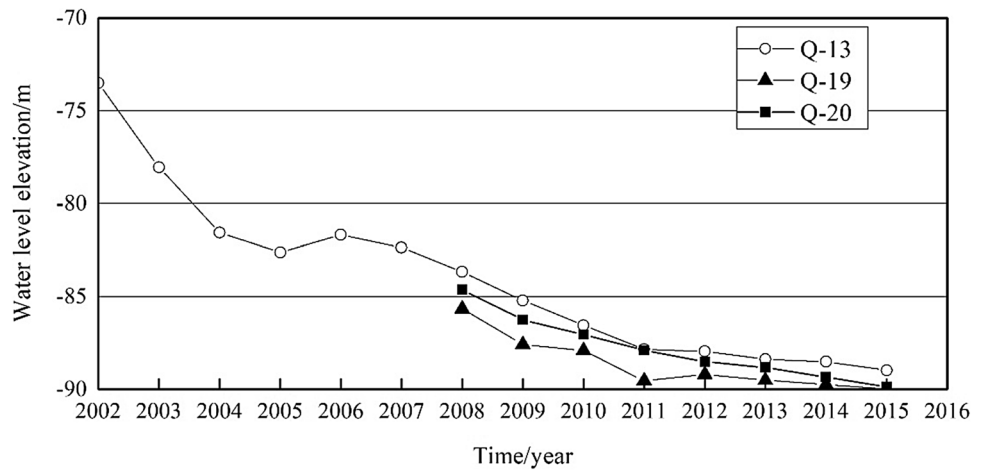
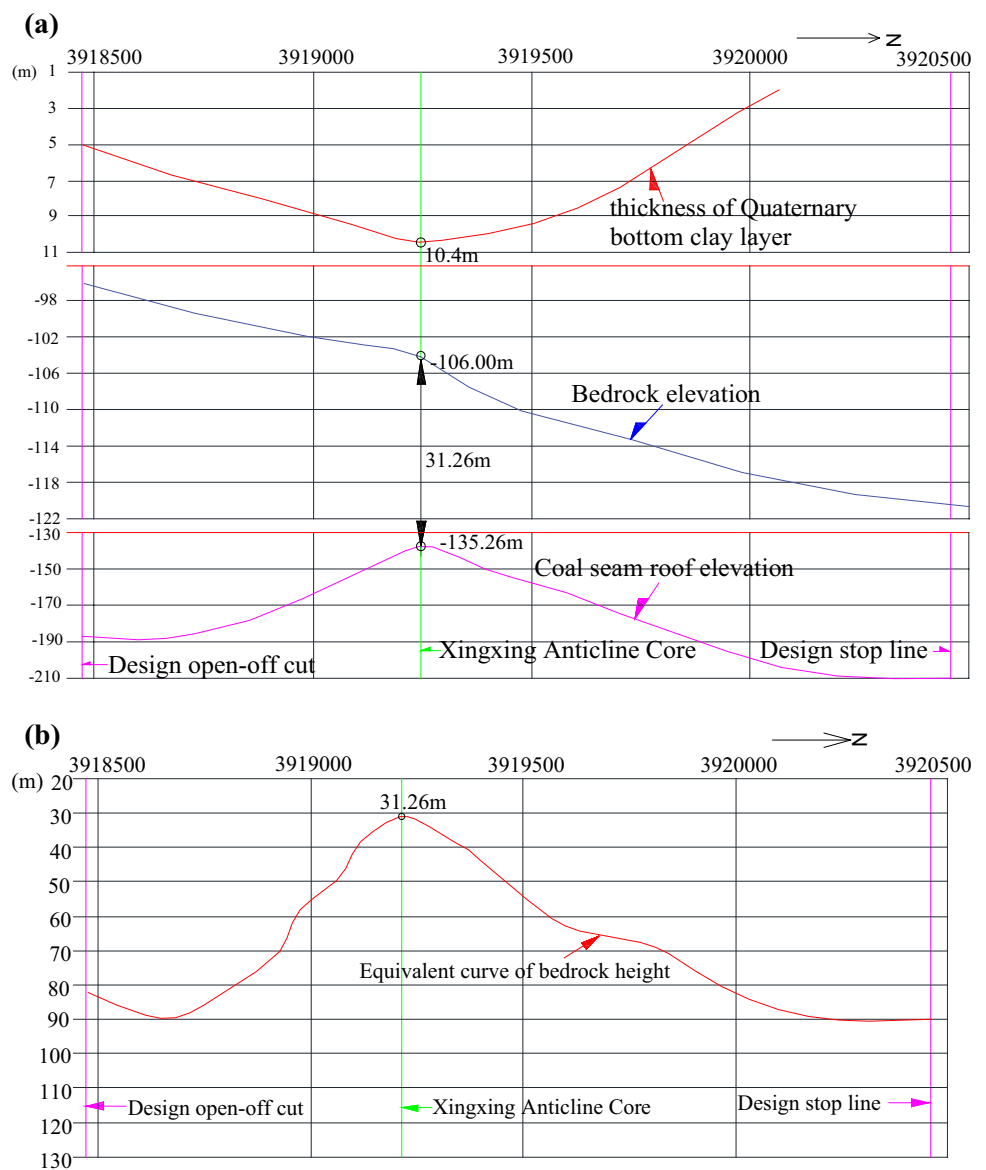


Fig. 4 Characteristic diagram of structure of overlying rock and soil in no. 1 exploration roadway: **a** Surface stratigraphy of bottom clay layer, bedrock elevation and coal seam roof in No.1 exploration roadway **b** Surface stratigraphy of bedrock in No.1 exploration roadway



Feasibility Analysis of Modifying Coal Pillars to Prevent Sand Flow

According to the above analysis, modification of coal pillars from those that prevent water seepage to those that prevent sand flow is deemed feasible in the No. 8 Mining District of the Baodian Coal Mine because of the low pressure and low water levels of the aquifers. Therefore, according to the mining regulations for the no. 3 coal seam, a coal pillar that prevents sand flow can be used to protect mines when the aquifers are weak, with low porosity, but only if the caved zone cannot affect those aquifers. Thus, the heights of the Two Zones in the first working face had to be analysed. Two methods were used to determine the heights of the Two Zones: numerical simulation with FLAC^{3D} software and comparative analysis based on field experience and observations.

Numerical Simulation Analysis

A numerical calculation of the deformation due to coal mining was performed, and the parameters of the Two Zones

were obtained from the workplace based on the combined conditions of the top and bottom rock strata, which are controlled by the first workface and nearby drilling in the no. 3 coal seam. The coal seam, roof, and floor were divided into seven types in accordance with the lithology and structure: limestone, fine sandstone interbedded with siltstone, fine sandstone, siltstone, sandy mudstone, mudstone, and coal (Table 1). The numerical model parameters were selected by using the measured data, which were obtained through the drilled holes. The combined structure consisted of 18 layers, which were the basis for establishing the engineering geological model.

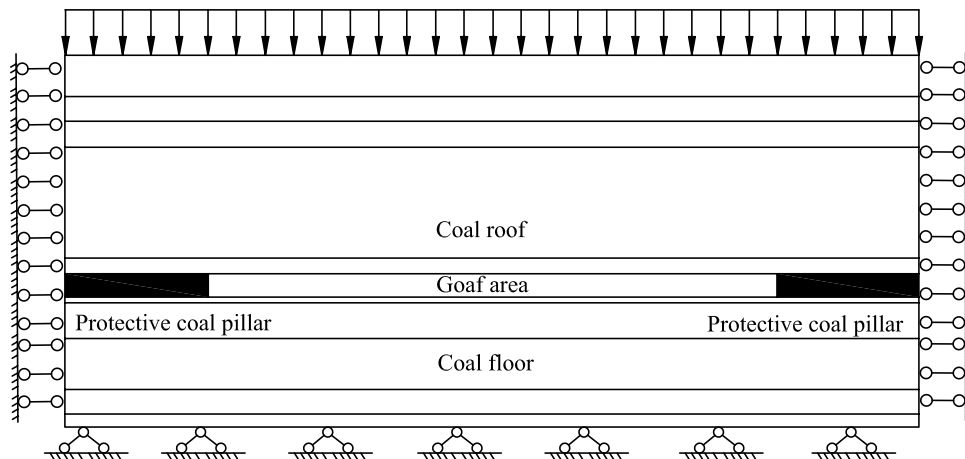
The length and width for the spatial range of the engineering geological model are 400 and 300 m, respectively, with a height of 174 m. Considering safety, the thickness of the mined coal seam is 7 m. The thickness of the upper strata is 104 m, and that of the lower strata is 63 m; the stress from the gravity of the overlying rock is 5.2 MPa (Fig. 5). Based on the calculations of the actual conditions, the boundary conditions are as follows:

1. The upper top boundary conditions are determined by the stress from the weight of the overburden. For con-

Table 1 Numerical model parameters

Rock formation	Elastic modulus (MPa)	Poisson’s ratio	Cohesion (MPa)	Internal friction angle (°)	Tensile strength (MPa)	Density (kg/m ³)
Fine sandstone interbedded with siltstone	1200	0.24	4.4	30	2.7	2500
Mudstone	660	0.28	2.0	27	1.6	2100
Sandy mudstone	780	0.28	2.3	27	1.7	2200
Siltstone	860	0.26	3.0	29	2.4	2300
Coal seam	400	0.30	0.8	22	0.6	1400
Fine sandstone	1100	0.25	3.4	31	2.5	2400
Limestone	1600	0.18	6.3	34	4.6	2700

Fig. 5 Numerical model of initial and boundary conditions

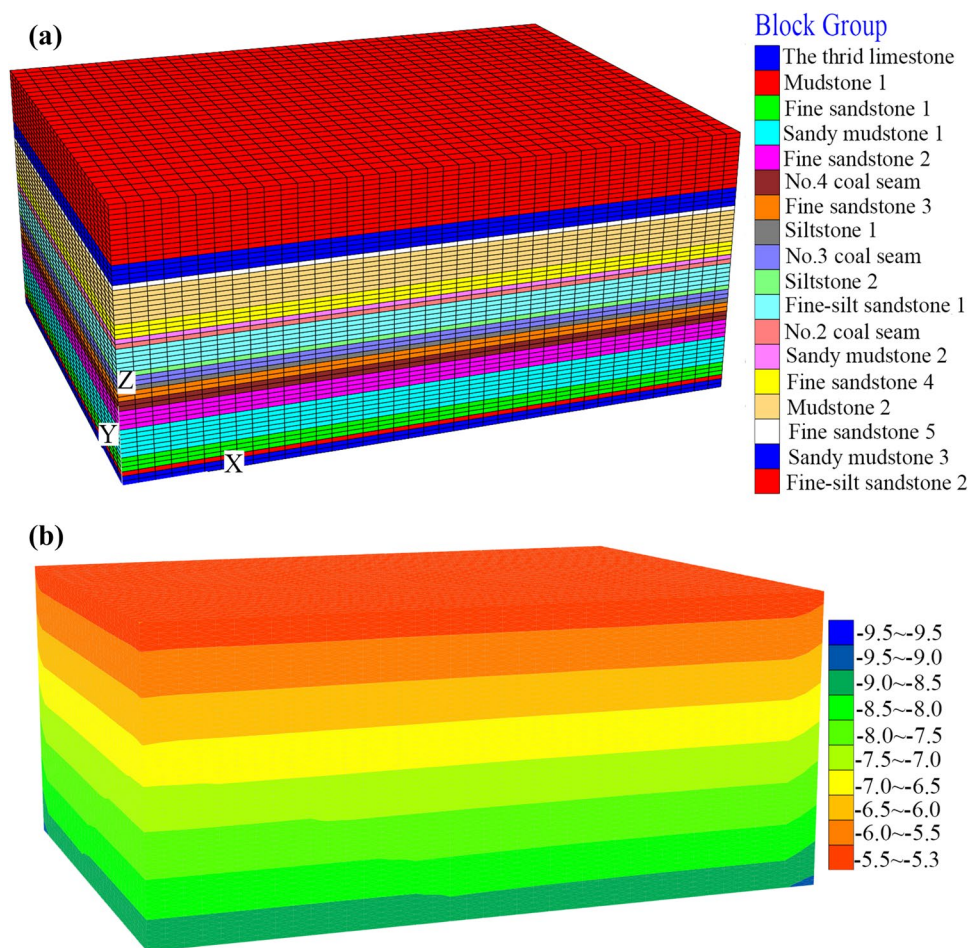


venience, the distribution of the load was simplified to a uniform load. The upper boundary conditions are the stress boundary conditions. The stress from 218 m of overburden is approximately 5.2 MPa.

2. The lower bottom boundary conditions of this model are the bottom plates, simplified as displacement boundary conditions. The model can move in the Y direction but not in the X direction.
3. The surrounding boundary conditions on both sides of this model are rock, simplified as displacement boundary conditions in that the model, which can move in the Y direction, but not in the X direction.

A three-dimensional model of the full-thickness work face was established with FLAC^{3D} software in accordance with the design plan for the workface. Arbitrary quadrilateral units were used to improve the accuracy of the calculations. The surrounding units in the mine were discretized and divided into 69,600 elements and 74,989 nodes (Fig. 6a). The initial pre-mining stress in the vertical direction was established (Fig. 6b) based on the geometric model and the physical–mechanical parameters of the rock strata.

Fig. 6 Numerical model and vertical stress distribution before mining: **a** Numerical model **b** Contour diagram of pre-mining vertical stress (MPa)



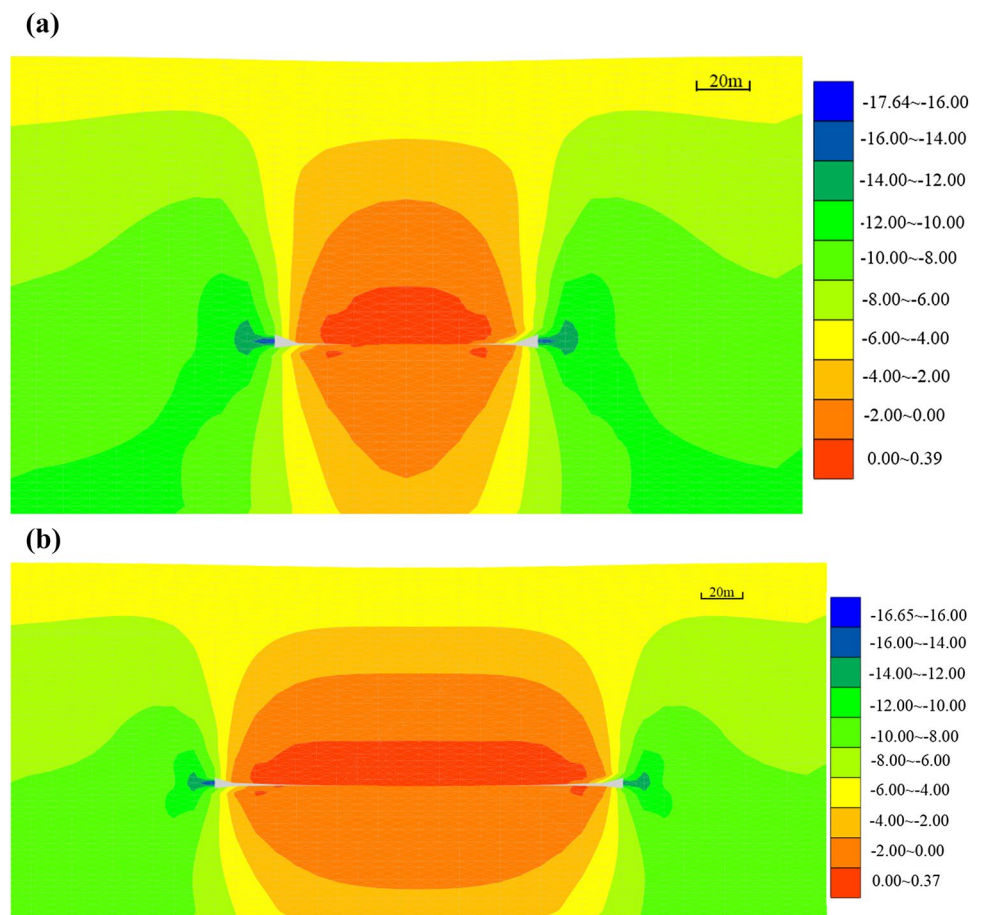
Stress Distribution After Mining

Figure 5 shows the contour diagrams of the vertical stress in the roof and floor after the first workface in the no. 3 coal seam was mined. The simulation of the stress distribution in the mine roof shows that as the workface advanced, vertical stress increased, leading to deterioration of the coal seam roof and formation of the Two Zones. The concentration of stress in the roof and bottom of the nearby workface substantially increased, causing a great amount of roof damage.

Mining of the coal seam changed the stress state of the rock near the workface; the stress was redistributed and concentrated in the coal seam and rock mass at both ends of the workface. Areas of reduced stress were produced in the rock mass above the workface. Finally, the entire vertical stress profile showed a “saddle-shaped” curve distribution.

The distribution of the vertical stress after mining in the strike and mining direction shows that areas with increasing stress occurred in the wall of the open cut and the end of the underground mine; the maximum stress was 17.6 MPa. At both ends of the two graphs in Fig. 7, the stress gradually recovers, which is shown by an increase in the length of the curve. Analysis of the figure shows that the mechanics

Fig. 7 Vertical stress distribution diagram of coal mine roof and bottom (MPa): **a** Trend of the vertical stress contour of a vertical longitudinal section **b** Typical vertical stress contour of a vertical longitudinal section



behind the stress increases are different: the stress increases in the wall are due to low rates of release of the strain energy during the mining process, which leads to accumulated strain energy (Fig. 7a). However, at the end of the workface, the strain energy cannot be released by workface advancement, which causes accumulation of strain energy during mining (Fig. 7b).

Roof Deterioration

According to the principles that govern mining stress (Lu 2018), the damaged zones that develop from top to bottom in the roof of the coal seam after mining include: an area without destruction and zones of shear failure, tensile fractures, and tensile damage. Shear yielding primarily takes place in the plastic zone, which occurs at the supporting wall in the goaf, and local tensile yielding emerges at the roof of the coal seam in the middle of the goaf. As both shear and tensile yielding occur on both sides of the workface, each side was subject to its effects (Fig. 8a). In contrast, tensile yielding is primarily found in the goaf at the middle of the work face. Shear yielding is primarily found in the plastic zone (Fig. 8b). Therefore, both sides of the workface are affected

by shear and tensile yielding. Tensile yielding is primarily found in the middle section of the workface.

According to the simulated results of roof deformation, the middle section of the first workface mainly suffers tensile yield failure and shear failure at both sides of the workface (Ma et al. 2010; Qian et al. 1994). The roof of the workface is saddle-shaped, and the height of the damage takes place near the wall of the open cut and the end of the underground mine. The distribution of the plastic zone and the location of the maximum plastic zone development in the roof are consistent with the distribution of stress in the roof during mining. The shear yielding zone of the roof appears to be slanted above and below the wall of the open cut and the end of the underground mine due to stress concentration in these areas. Although the largest stress zone is not close to the coal seam, a shear yield zone still emerges in the front and back of the workface due to the poor physical and mechanical properties of the coal seam.

Numerical Simulation Results

The plastic zone can be used to determine the height of the roof damage in accordance with the saddle shaped damage to the roof after mining. The heights of the Two Zones

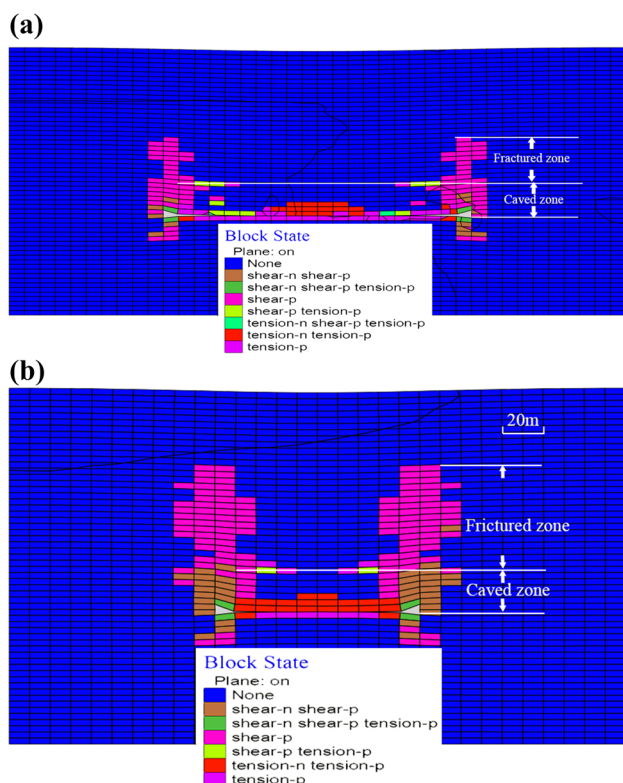


Fig. 8 Distribution of the plastic zone: **a** Trend of the plastic zone **b** Development of plastic zone

can be preliminarily determined by examining the amount of deformation in the simulation. The height of the caved zone is ≈ 21 m and the maximum height of the water-flow-fractured zone is ≈ 69 m.

Numerical simulation is an efficient method to provide insights into various problems. Numerical modelling can handle realistic problems with complex conditions. Conditions that cannot be experimentally examined in the field can also be applied. Numerical simulation can also perform stress and displacement analyses for each area and measurement point. However, the boundary conditions and material properties in numerical simulations are often simplified for analysis, which affects the results. Therefore, we compared the results of the numerical simulations with predictions based on empirical formulas.

Comparative Analysis of Empirical Formulas for the Two Zones

Height of the Caved Zone

According to research on modifying coal pillars to prevent sand flow rather than water seepage in the Xinglongzhuang Coal Mine, which is adjacent to the Baodian Coal Mine, the height of the caved zone is generally 3–4 times thicker than

the thickness required for conducting fully mechanized cave mining. In the present study, a mined thickness that was four times that required was used. Therefore, the formula for the height of the caved zone is:

$$H_K = 4 \times \sum M \quad (1)$$

where H_K is the height of the caved zone and $\sum M$ is the accumulated mined thickness.

Height of the Water-Flow-Fractured Zone

According to a geological report from the Yanzhou Coal Mine Co. (Huang 2007), the relationship between the maximum height of the water-flow-fractured zone and the mined thickness for performing fully mechanized cave mining is:

$$H_L = \frac{100 \sum M}{0.94 \sum M + 4.31} \pm 7.7 \quad (2)$$

where H_L is the height of the water flow fractured zone.

Results of Comparisons Based on Field Experience and Observations

The mined thickness is considered to average 5.8 m, and the heights of the Two Zones were determined using Eqs. (1) and (2), which yield values of 23.2 and 67.1 m, respectively.

Analysis of Coal Pillar Height to Prevent Sand Flow

Determining the Thickness of the Protective Layer

According to the characteristics of the overburden rock and soil body in the first workplace, the thickness of the protective layer was set at 1.5 times the average mined thickness, which is ≈ 5.8 m. Therefore, the maximum thickness of the protective layer is ≈ 8.7 m. The height of the caved zone was set at 23.2 m, so the height of the coal pillar to safely prevent sand flow would be 31.9 m.

Safety Analysis

Drilling data for the thinnest part of the bedrock and the thickest part of the coal seam were used for analysis (see Table 2) based on distribution of the bedrock thickness in the first workplace. Table 2 shows that the height of the coal pillar that would prevent sand flow in the thinnest part of the bedrock and thickest part of the coal seam was 28.5 and 36.3 m, respectively; both heights are less than the actual height of the coal pillar.

According to the numerical simulation results for the first workplace, the maximum height of the caved zone is found

Table 2 Comparison of thinnest part of bedrock with thickest part of coal seam for coal pillar that prevent sand flow

	Thickness of coal seam/m	Height of caved zone/m	Height of protective layer/m	Height of coal pillar that would prevent sand flow/m	Thickness of bedrock/m
Thinnest part of bedrock	5.17	20.7	7.8	28.5	31.26
Thickest part of coal seam	6.60	26.4	9.9	36.3	110.0

at the wall of the open cut and the end of the underground mine, and the thickness of the bedrock exceeds 80 m. As the height of the caved zone is considered using its maximum value, the thinnest part of the bedrock is at a greater distance from the wall of the open cut mine, so the actual height is less than the expected value. However, the bottom clay layer and weathered bedrock zones in the thinner part of the bedrock in the first workface are extremely favourable for preventing water and sand inrush. The stratigraphic composite of the structure cannot only reduce damage to the roof due to mining, but also inhibit the development of hydraulic fractures and compensate for issues caused by the thin bedrock. Therefore, our results justify the proposed modification of the coal pillar to one that prevents sand flow to increase the amount that can be safely mined.

Conclusions

The regularity of the bedrock was analysed by considering the effects of the geological structure and the relationship between the bedrock and the bottom clay layer, based on drilling data from the No. 8 Mining District, the stratigraphy of the bedrock, and a comparison of the heights of the bottom clay layer, bedrock, and coal seam roof in the first exploration roadway. Changes in the hydrogeological conditions were also analysed. The results led to the conclusion that it was feasible to modify the coal pillars from those that prevent water seepage to those that prevent sand flow.

An engineering geological model of the first workface was established. FLAC^{3D} software was used to determine the vertical stress distribution in the plastic zone and the heights of the Two Zones were obtained by examining the amount of deformation. The height of the caved zone was ≈ 21 m, and the maximum height of the water-flow- fractured zone was ≈ 69 m.

The heights of the Two Zones were also empirically calculated for a mined thickness of 5.8 m; they were 23.2 and 67.1 m, respectively. These results are in good agreement with those of the numerical simulation (21 and 69 m). For safety reasons, the higher values of 23.2 and 69 m were used as the heights of the Two Zones, respectively.

A comparison of the drilling data and the heights of the Two Zones shows that the height of the coal pillars that

would prevent sand flow at the thinnest part of the bedrock and the thickest part of the coal seam in the first workface was 28.5 and 36.3 m, respectively. Thus, the results validate the use of coal pillars to prevent sand flow to increase the area that can be safely mined.

Acknowledgements This research was supported by the Fundamental Research Funds for the Central Universities (No. 2015XKMS035), National Natural Science Foundation of China (41727801, 41741020), and the Priority Academic Program Development of Jiangsu Higher Education Institutions (PAPD).

References

Baumann T, Bartels J, Lafogler M, Wenderoth F (2017) Assessment of heat mining and hydrogeochemical reactions with data from a former geothermal injection well in the Malm Aquifer, Bavarian Molasse Basin, Germany. *Geothermics* 66:50–60

Bense VF, Van Balen D, Van den Berg EH (2003) Deformation mechanisms and hydraulic properties of fault zones in unconsolidated sediments; the Roer Valley Rift System, the Netherlands. *Hydro J* 11(3):319–332

Bertuzzi R, Douglas K, Mostyn G (2016) An approach to model the strength of coal pillars. *Int J Rock Mech Min Sci* 89:165–175

Fang XQ, Huang HF, Jin T, Bai JB (2007) Strata behavior of fully-mechanized top coal caving in thin bedrock and thick topsoil. *J Min Saf Eng* 24(3):326–330 (In Chinese)

Feng SJ, Sun SG, Lv YG, Lv J (2011) Research on the height of water flowing fractured zone of fully mechanized caving mining in extra-thick coal seam. *Procedia Eng* 26:466–471

Hang Y, Zhang GL, Yang GY (2009) Numerical simulation of dewatering thick unconsolidated aquifers for safety of underground coal mining. *Min Sci Tech* 19(3):312–316 (In Chinese)

Huang FC (2007) Subsidence control and treatment technology of fully-mechanized cave mining in a thick coal seam. Coal Industry Press, Beijing (In Chinese)

Jin DW, Zheng G, Liu ZB, Liu YF, Pang XQ (2011) Real-time monitoring and early warning techniques of water inrush through the coal floor. *Procedia Earth Planet Sci* 3:37–46

Li B, Chen YL (2016) Risk assessment of coal floor water inrush from underlying aquifers based on GRA-AHP and its application. *GEGE* 34(1):143–154

Liu DS, Guo DW (2000) Study on engineering geology of preventing sand and rock pillar under thick alluvium. *Shandong Coal Sci Tech* 3:17–20 (In Chinese)

Liu Y, Chai XZ, Li JS (2009) Study on optimization of waterproof coal and rock pillar in adjacent coal faces. *J China Coal Soc* 34(2):239–242 (In Chinese)

Lu CZ (2018) The analysis of the stress distribution characteristics of composite roof structure surface in coal mining. *Energ Energy Conserv* 2:44–45 (In Chinese)

- Lu YL, Wang LG (2015) Numerical simulation of mining-induced fracture evolution and water flow in coal seam floor above a confined aquifer. *Comput Geotech* 67:157–171
- Ma SM, Lv WY, Sun BY (2010) Research status and trend of mining pressure theory in deep stope. *Coal Eng* 10:87–89 (**In Chinese**)
- Palchik V (2002) Influence of physical characteristics of weak rock mass on height of caved zone over abandoned subsurface coal mines. *Environ Geo* 42:92–101
- Poulsen BA, Shen B, Williams DJ, Huddleston-Holmes C, Erarslan N (2014) Strength reduction on saturation of coal and coal measures rocks with implications for coal pillar strength. *Int J Rock Mech Min Sci* 71:41–52
- Qian MG, He FL, Wang ZT, Gao CB (1994) Rediscovery on mine pressure theory of stope. *J China U Min Technol* 23(3):1–9 (**In Chinese**)
- Reed G, Mctyer K, Frith R (2017) An assessment of coal pillar system stability criteria based on a mechanistic evaluation of the interaction between coal pillars and the overburden. *Int J Min Sci Tech* 27(1):9–15
- Sun WJ, Wang YW, Li XK, Yang WK, He YC (2015) Mine hydrogeology type and water hazard accident analysis in north China coalfield. *Coal Eng* 47(6):103–105 (**In Chinese**)
- Waclawik P, Ptacek J, Konicek P, Kukutsch R, Nemcik J (2016) Stress-state monitoring of coal pillars during room and pillar extraction. *J Sustainable Min* 15(2):49–56
- Wei JC, Wu FZ, Yin HY, Guo JB, Xie DL, Xiao LL, Zhi HF, Lefticariu L (2017) Formation and height of the interconnected fractures zone after extraction of thick coal seams with weak overburden in western China. *Mine Water Environ* 36(1):59–66
- Wen L, Yao DX, Lu HF (2013) Feasibility study of preventing sand pillar in safe mining of coal seam near loose aquifer. *Coal Geo Cn* 25(6):43–45 (**In Chinese**)
- Wu Q, Dong DL, Qian ZJ, Guan ET, Li SW (2000) On the geological structure theory of three—dimensional water filling in north China type coalfields. *J China Coal Soc* 2:47–49 (**In Chinese**)
- Wu J, Jiang ZQ, Zhai XR (2011) Research on controlling of rock mass structure on water inrush from coal seam floor in Huaibei mining area. *Procedia Eng* 26:343–350
- Wu JS, Xu SD, Zhou R, Qin YP (2016) Scenario analysis of mine water inrush hazard using Bayesian networks. *Safety Sci* 89:231–239
- Xu DJ, Peng SP, Xiang SY, Liang M, Liu W (2016) The effects of caving of a coal mine’s immediate roof on floor strata failure and water inrush. *Mine Water Environ* 35(3):337–349
- Yang WF, Xia XH (2013) Prediction of mining subsidence under thin bedrock and thick unconsolidated layers based on field measurement and artificial neural networks. *Comput Geosci* 52:199–203
- Zhang DS, Fan GW, Liu YD, Ma LQ (2010) Field trials of aquifer protection in longwall mining of shallow coal seams in China. *Int J Rock Mech Min Sci* 47(6):908–914
- Zhang YG, Zhu SY, Li YJ, Liu YX, Wu YL (2017) Study on type change of coal pillar setting under thin Bedrock with thick loose bed. *Coal Technol* 36(5):63–65 (**In Chinese**)
- Zhao YL, Luo SL, Wang YX, Wang WJ, Zhang LY, Wan W (2017) Numerical analysis of karst water inrush and a criterion for establishing the width of water-resistant rock pillars. *Mine Water Environ* 36(4):508–519
- Zhu HZ, Liu P, Tong ZY (2014) Numerical simulation research and application on protected layer pressure relief affection under different coal pillar width. *Procedia Eng* 84:818–825